Ortho-imaging and RTP Model Panning Considerations for Airborne and Spaceborne Linear Array Imagery

Azubuike G. Nwosu
Department of Civil Engineering, University of Benin, Benin-city, Nigeria

Raphael Ehigiator-Irughe
Department of Geomatics, University of Benin, Benin-city, Nigeria

Jacob Ehiorobo
Department of Civil Engineering, University of Benin, Benin-city, Nigeria

DOI: https://doi.org/10.56293/IJASR.2025.6318

IJASR 2025
VOLUME 8
ISSUE 1 JANUARY - FEBRUARY **ISSN: 2581-7876**

Abstract: For spaceborne and airborne linear array imagery, there are computational protocols for ortho-image generation, with different variations for visualisation projects (input-driven computation) and conventional mapping (output driven computation), and the latter may include the use of anchor-points in the image to ease the computational load. Similarly, there are algorithms for real-time model panning, with options that mitigate limitations imposed by computational circumstances, and this would include the use of Rational Polynomial Coefficients (RPCs). A good geometric camera model is needed to support production lines that utilise linear array imagery and the derivations are presented in detail, followed by the algorithms for ortho-imaging and real time model panning.

Keywords: Linear array; RTP; Ortho-imaging; SPOT; ASAS.

I. INTRODUCTION

Optimised camera models have been developed for both spaceborne SPOT imagery and airborne ASAS (Advanced Solid-state Array Spectroradiometer).

A camera model defines the geometry of a camera based on orientation parameters. Orientation based on such a model, when calculated for stereo imagery, would allow for the computation of the co-ordinates of conjugate points in the images and, eventually, the generation of a digital terrain model (DEM). Orientation parameters are also used to resample the image to correct for relief displacement and produce an ortho-image. Resampling need not rely on a DEM computed from the stereo imagery because a DEM may be available in a database. Thus, the most important need for a camera model is to ortho-correct an image for extraction of features into a geo-database.

Real Time Photogrammetry is vital for the accomplishment of many tasks. The continuing improvement in the performance of computing systems allows for improvements to be made in the performance of real time systems. Real time photogrammetry tends to be discussed in two contexts:

Case 1: Real time stereo model panning. This refers to the use of orientation parameters of stereo imagery to move automatically to conjugate points on a stereo pair for extraction of terrain features, usually in a photogrammetric plotter. It is usually referred to as "on-line aspects".

Case 2: Instantaneous processing of imagery with orientation data collected during image-data acquisition. This would allow for an ortho image to be computed immediately in an aircraft and recorded. This is still a continuing research issue with a lot of technical and logistic bottlenecks for linear array systems. The nature of linear array images, with lines of continuously changing orientation, compounds the problem enormously. The test models

utilising INS data have contributed to achieving this possibility. The major problems are the accuracy and frequency of measurements of orientation data, and their proper filtering.

One section here and deals with considerations and techniques for ortho-resampling of imagery, the other with the setup of real-time model panning computations. The other section discusses "on-line aspects" to implement real-time panning in photogrammetry. Before these two, you need a good camera model.

II. MATERIALS FOR THE CAMERA MODEL

Imagery of SPOT satellite data of Aix-en-Provence, France was made available covering the test area of European Organisation for Experimental Photogrammetric Research (OEEPE) with long-signalised ground control points. The Biospherics department of NASA Goddard Space Flight Centre provided ASAS airborne data via a research partnership. This covers area of Maricopa, Arizona, with 29 spectral bands, seven pointing angles, and supported by a 5Hz Inertial Navigation System (INS). ASAS [1] is the Advanced Solid-State Array Spectroradiometer.

III. METHODS FOR THE CAMERA MODELS

A geometric camera model is simply a mathematical representation of a line from a point on the camera image, passing through the centre of the camera-lens, to the feature it captures on the imaged surface. Several equations of these lines could be used to compute / refine the orientation parameters of an image.

SPOT camera modelling: For spaceborne SPOT, control information is in a local co-ordinate system. There are three rotations in the mathematical model to transform to geographical co-ordinates, to the ECEF, and to the ECI system for use in this model. This model merges the earth-centred inertial geocentric co-ordinate system (ECI) and the the earth-centred, earth-fixed geocentric system (ECEF), but transformations are required between these other systems.

$$\mathbf{Xg} = \mathbf{Xs} + \Delta \, Ri \, Rb \, Rs \, \mathbf{xÞ} \quad (1)$$

where

i. **xÞ** = image co-ordinates vector
ii. Xg = ground co-ordinates vector in ECI
iii. Xs = satellite position vector in ECI
iv. Δ = scale factor
v. Ri = Rotation from the orbital reference system to the ECI
vi. Rb = Rotation between the attitude reference system and the orbital system.
vii. Rs = Rotation between the sensor and the attitude reference system

The reverse equation is:

$$\mathbf{xÞ} = 1/\Delta \, . \, R \, . \, \mathbf{(Xg - Xs)} \quad (2)$$

where R = (Rs . Rb . Ri)

In matrix form, this becomes:

$$\begin{bmatrix} 0 \\ y_p \\ -c \end{bmatrix} = \frac{1}{\Delta} \begin{bmatrix} r_{11} & r_{12} & r_{13} \\ r_{21} & r_{22} & r_{23} \\ r_{31} & r_{32} & r_{33} \end{bmatrix} \bullet \begin{bmatrix} Xg - Xs \\ Yg - Ys \\ Zg - Zs \end{bmatrix} \quad (3)$$

y_p is the y-image co-ordinate, and c is the focal length of the camera.

The 8 parameters of orientation to be corrected are:

[I_o, Ω_o, t_o, r_o, ω_o, ρ_o, κ_o, ρt_o].

ρto is the linear component of the phi rotational parameter. The others are Inclination (I),

Right Ascension (Ω), Time at Ascending node (t_o), Orbital radius at Ascending node (r_o).

A Taylor's series expansion of the collinearity equations is done but only the first order terms are taken.

$$A_k = \begin{bmatrix} \frac{\delta F_1}{\delta y_p} & \frac{\delta F_1}{\delta t} & \frac{\delta F_1}{\delta \varphi} & \frac{\delta F_1}{\delta \lambda} & \frac{\delta F_1}{\delta h} \\ \frac{\delta F_2}{\delta y_p} & \frac{\delta F_2}{\delta t} & \frac{\delta F_2}{\delta \varphi} & \frac{\delta F_2}{\delta \lambda} & \frac{\delta F_2}{\delta h} \end{bmatrix} \quad (4)$$

$$B_k = \begin{bmatrix} \frac{\delta F_1}{\delta I} & \frac{\delta F_1}{\delta \Omega} & \frac{\delta F_1}{\delta t_o} & \frac{\delta F_1}{\delta r_0} & \frac{\delta F_1}{\delta w_o} & \frac{\delta F_1}{\delta \rho_0} & \frac{\delta F_1}{\delta \kappa_0} \\ \frac{\delta F_2}{\delta I} & \frac{\delta F_2}{\delta \Omega} & \frac{\delta F_2}{\delta t_o} & \frac{\delta F_2}{\delta r_0} & \frac{\delta F_2}{\delta w_o} & \frac{\delta F_2}{\delta \rho_0} & \frac{\delta F_2}{\delta \kappa_0} \end{bmatrix} \quad (5)$$

The condition equation can be written as:

$$Av + B\xi = f \quad (6)$$

where v is the vector of measurement residuals, ξ are the corrections to parameters which are initially given as approximate values. This could be reformulated for computational stability [2] [3] to avoid correlation between phi attitude parameter and platform motion.

$$\begin{bmatrix} A & 0 \\ 0 & I \end{bmatrix} \begin{bmatrix} v \\ v_p \end{bmatrix} + \begin{bmatrix} B \\ -I \end{bmatrix} \xi = \begin{bmatrix} c \\ 0 \end{bmatrix} \quad (7)$$

The solution by [4] is:

if **Q** is the apriori cofactor matrix for the measurements

and **Wpp** is the apriori weight matrix for the parameter estimates. Then,

$$\xi = (B^T (AQA^T)^{-1} B + W_{pp})^{-1} B (AQA^T)^{-1} f \quad (8)$$

v can always be calculated after a convergence has been achieved from a few iterations.

$$v = A^T (AQA^T)^{-1} (f - B\xi) \quad (9)$$

This SPOT model converges in 3 or 4 iterations;

beyond 5 iterations is usually a sign of a poor GCP configuration, or deficient modelling.

ASAS camera modelling: The is an airborne camera, so equation linking the image co-ordinates to the ground co-ordinates of a GCP is given by the direct collinearity equation as utilised for the SPOT system above, but here we have only one set of rotations. With ASAS the model includes 2nd degree polynomials of camera position as well as camera attitude angles, to compensate for its turbulent platform. Here x_p is used in place of elapsed time.

$$X_s = X_{s0} + X_{s1} . x_p + X_{s2} . x_p . x_p \quad (10)$$

$$Y_s = Y_{s0} + Y_{s1} . x_p + Y_{s2} . x_p . x_p \quad (11)$$

$$Z_s = Z_{s0} + Z_{s1} . x_p + Z_{s2} . x_p . x_p \quad (12)$$

R = f (kappa, phi, omega)

$$\text{Kappa} = \kappa + \kappa_1 . x_p + \kappa_2 . x_p . x_p \quad 15)$$

$$\text{Phi} = \varphi + \varphi_1 . x_p + \varphi_2 . x_p . x_p \quad (16)$$

$$\text{omega} = \omega + \omega_1 . x_p + \omega_2 . x_p . x_p \quad (17)$$

x_p = line-number * CID-element-size-in-y /2

Here, element size-in-y is used instead of x, and scaled down for stability.

y_p is the y-image co-ordinate, and c is the focal length of the ASAS camera. There is only one set of rotations attitude angles.

$$R = \begin{bmatrix} \cos k & \sin k & 0 \\ -\sin k & \cos k & 0 \\ 0 & 0 & 1 \end{bmatrix} \cdot \begin{bmatrix} \cos\varphi & 0 & \sin\varphi \\ 0 & 1 & 0 \\ -\sin\varphi & 0 & \cos\varphi \end{bmatrix} \cdot \begin{bmatrix} 1 & 0 & 0 \\ 0 & \cos\omega & \sin\omega \\ 0 & -\sin\omega & \cos\omega \end{bmatrix} \quad (18)$$

Since they would not be error free, the adjustment could compute corrections (residuals) for the five observations x-image, y-image co-ordinate, Eastings (E), Northings (N) and Height (h). $[x_p, y_p, E, N, h]$

There are 15 parameters, which include linear and polynomial parameters of orientation to be corrected. Phi is fixed to the value of the pointing angle and, with its linear and polynomial components dropped from the model, leaving:

$$[\kappa_0, \omega_0, \kappa_1, \omega_1, \kappa_2, \omega_2, X_0, Y_0, Z_0, X_1, Y_1, Z_1, X_2, Y_2, Z_2] \quad (19)$$

A Taylor's series expansion of the collinearity equations is done but only the first order terms are used. The matrix takes this form in equation (20) and (21).

$$A_k = \begin{bmatrix} \frac{\delta F_1}{\delta \kappa_0} & \frac{\delta F_1}{\delta \omega_0} & \frac{\delta F_1}{\delta \kappa_1} & \frac{\delta F_1}{\delta \omega_1} & \frac{\delta F_1}{\delta \kappa_2} & \frac{\delta F_1}{\delta \omega_2} & \frac{\delta F_1}{\delta X_0} & \frac{\delta F_1}{\delta Y_0} & \frac{\delta F_1}{\delta Z_0} \cdots \\ \frac{\delta F_2}{\delta \kappa_0} & \frac{\delta F_2}{\delta \omega_0} & \frac{\delta F_2}{\delta \kappa_1} & \frac{\delta F_2}{\delta \omega_1} & \frac{\delta F_2}{\delta \kappa_2} & \frac{\delta F_2}{\delta \omega_2} & \frac{\delta F_2}{\delta X_0} & \frac{\delta F_2}{\delta Y_0} & \frac{\delta F_2}{\delta Z_0} \cdots \end{bmatrix} \quad (20)$$

$$B_k = \begin{bmatrix} \frac{\delta F_1}{\delta y_p} & \frac{\delta F_1}{\delta x_p} & \frac{\delta F_1}{\delta E} & \frac{\delta F_1}{\delta N} & \frac{\delta F_1}{\delta H} \\ \frac{\delta F_2}{\delta y_p} & \frac{\delta F_2}{\delta x_p} & \frac{\delta F_2}{\delta E} & \frac{\delta F_2}{\delta N} & \frac{\delta F_2}{\delta H} \end{bmatrix} \quad (21)$$

Where n is the number of GCPs. The condition equation can be written as:

$$Av + B\xi = f \quad (22)$$

Similarly to SPOT, the solution by [4] is used as shown in the previous section.

IV. TEST RESULTS OF MODELS

A. SCENARIO 1 SPOT ORBIT MODEL WITH LINEAR PHI.

Added refinements is the addition of a linear-phi parameter which was found to be significant during simulations and resulted in improved performance with a total of 8 parameters.

Table 1: Experiment 1 scenario 1 SPOT Orbit model with linear phi

No of GCPs	No of chk-points	RMSE GCPs (pix)	RMSE chk- points (pix)
18	0	0.97	nil
14	4	0.89	1.3
10	8	0.75	1.25
7	11	0.51	1.40

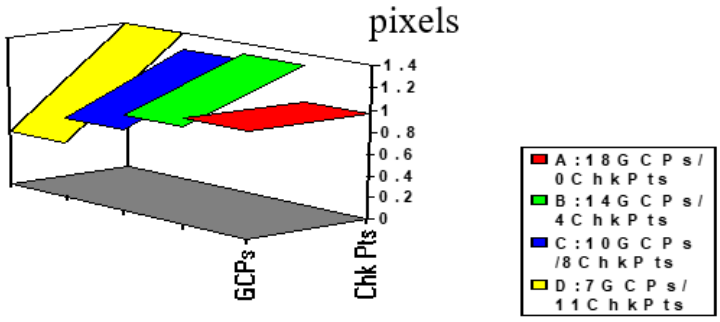

Figure 1. scenario 1 SPOT Orbit model with linear phi

B. SPOT SCENARIO 2 MERGING ECEF AND ECI

Some generic facilities were introduced to seek wider application of the model to both airborne and space-borne systems, resulting in a further simplified model. The solution is still orbital, but it is assumed that during the period of imaging a spot scene, the ECEF and ECI system coincide, so there is no need to transform to-and-from the orbital system. The parameters remain the same for a total of 8. Computations were slightly faster here because of the absence of inertial transformations. This shows a slight improvement on the full Orbit model, despite using a less complex algorithm with less computational load.

Table 2: scenario 2 merging ECEF and ECI

No of GCPs	No of checkPts	RMSE GCPs (pix) with tiepoints without tiepoints	RMSE chkPts (pix)
17	0	0.92 0.92	nil
13	4	0.90 0.86	0.99 1.01
11	6	0.83 0.92	1.27 0.85
9	8	0.80 0.75	1.36 0.89
	10	0.78 0.73	1.25 1.35

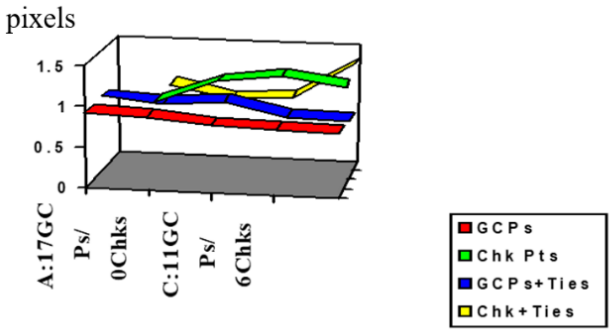

Figure 2: Experiment 1 scenario 4 merging ECEF and ECI

C. SCENARIO 3 ASAS MODEL WITH ONLY GCPS

With 15 parameters and only 10 GCPs, it was not possible to isolate some points to use as checkpoints. The model converged very well in a few iterations, rendering sub-pixel accuracy, confirming the possibility of modelling the effects of linearly changing camera positions. Test results further showed that deviations away from GCPs was up to four Table 7: Experiment 1 scenario 1 on ASAS with GCPs

Table 3: Experiment 1 scenario 1 on ASAS with GCPs

View No	Pointing angl- degs	RMSE -X pix	RMSE -Y pix	RMSE -XY pix
1	45.0	1.685	0.429	1.057
2	29.5	1.091	0.532	0.812
4	0.0	1.160	0.709	0.939

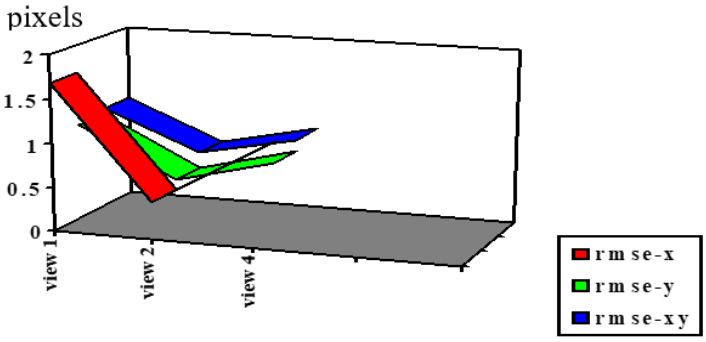

Figure 3: Scenario 3 ASAS model with only GCPs

The geometric quality of an ASAS view may not be predictable because a lot depends on platform stability during the flight, and this determines the quality of resection. With similar platform turbulence, views nearer the vertical are better; but in this case view 2 has outperformed view 4.

D. SCENARIO 4 ASAS MODEL WITH GCPS AND INS

Full INS support is just for orientation but GCPs are used for refinement (or calibration). 9 parameters are corrected, 3 for attitude and 6 for platform position because of the presence of drift errors in the later.

The GCP field seemed to be weak, with some showing high residuals. There were much higher residuals in X-flight direction than in Y- due to the method of computation and because INS measurements are modelled with image line-numbers; time synchronisation errors will normally show up in X.

Table 4: scenario 2 ASAS model with INS and GCPs

View No	Pointing Angl degs	RMSE-X pixel	RMSE-Y pixel	RMSE-XY pixel
2	30	5.25	2.01	3.63
4	0	2.19	0.72	1.46

The orientation relies solely on INS data but GPPs are used for refinement (calibration). When corrected for the precision of GCPs and point identification on the ASAS images, these residuals would be lower, but results show that the 1Hz INS used here is not adequate.

V. ALGORITHM FOR ORTHO-IMAGE PRODUCTION

An ortho-image can be generated by using a geometric camera model and a digital elevation model (DEM) of the target area. In the absence of a DEM, other height information, e.g. contours, can be processed into a DEM or a Digital Terrain Model – DTM [5]. The target area would usually be a sub-image delineated by ground or image co-ordinates. A DTM is a DEM to which terrain features, like break-lines, have been added for better representation of the surface.

A. INPUT DRIVEN RESAMPLING

If the target area was defined in image co-ordinates, this could force the use of an input driven system. This is calculated with the inverse photogrammetric equations shown below. The area to be resampled and the resolution is given in image units.

inverse equations

$$X_i - X_0 = (Z_i - Z_0)\frac{r_{21}\cdot y_1 - r_{31}\cdot c}{r_{23}\cdot y_1 - r_{33}\cdot c} \qquad (23)$$

$$Y_i - Y_0 = (Z_i - Z_0)\frac{r_{22}\cdot y_1 - r_{32}\cdot c}{r_{23}\cdot y_1 - r_{33}\cdot c}$$

X_i, Y_i, Z_i are ground coordinates of an image point

X_o, Y_o, Z_o are ground coordinates of the camera position at the time of imaging

This requires a tracing of the collinearity ray from the image to the ground as articulated by [6]. For a linear array camera model, orientation is derived for each line of imagery and need not be determined by iteration in this method - this is an advantage. However, since the ground is not a plane, the ray tracer would rely on a DEM and an iterative solution in the DEM system. This has attendant disadvantages, for example, many number of iterations may be needed for convergence, reducing performance and with a higher risk of failure. Besides, gaps may occur in the output and must be interpolated, because airborne linear arrays are prone to over-sampling and under-sampling.

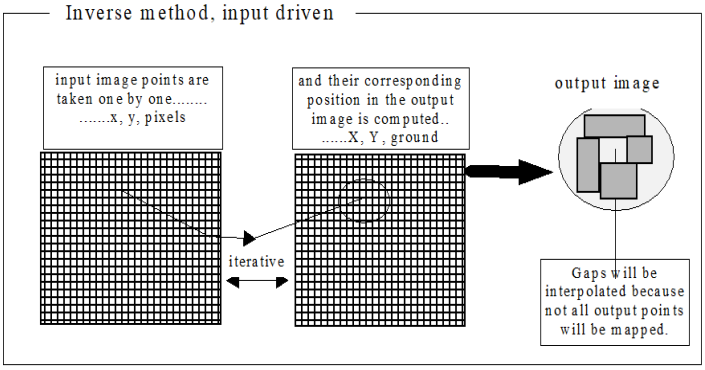

Figure 4: Inverse method ortho-computation

Imagery re-sampled for visualisation would normally use the input driven system because the visualisation path is usually defined as a set of camera positions and view directions.

A resampling method for SPOT imagery has been presented by [7] using anchor points for fast generation of SPOT ortho-images. This approach was motivated by limitations in computer processing speed. These limitations may still be relevant in some cases, but imagery could be processed fully taking advantage of substantial gains in performance by computing systems in the last several years.

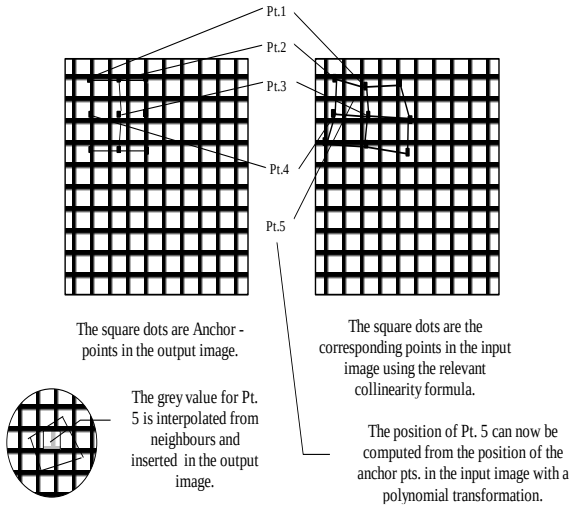

Figure 5: Rectification by Anchor-points

B. OUTPUT DRIVEN RESAMPLING

If the target area was defined in ground co-ordinates, an input driven system is used. This is calculated with the direct equations shown below.

direct equations

$$0 = -c \bullet \frac{r_{11}(X_g - X_0) + r_{12}(Y_g - Y_0) + r_{13}(Z_g - Z_0)}{r_{31}(X_g - X_0) + r_{32}(Y_g - Y_0) + r_{33}(Z_g - Z_0)}$$

$$y_p = -c \bullet \frac{r_{21}(X_g - X_0) + r_{22}(Y_g - Y_0) + r_{33} Z_g - Z_0)}{r_{31}(X_g - X_0) + r_{32}(Y_g - Y_0) + r_{33}(Z_g - Z_0)} \quad (24)$$

X_g, Y_g, Z_g are ground coordinates of an image point

X_o, Y_o, Z_o are ground coordinates of the camera position at the time of imaging

The area to be resampled and the resolution is given in ground units. This resampling resolution is then used to rasterise the project area into cell points. Where the project area is rectangular, it is only necessary to store the ground co-ordinates of the origin, the ground sampling resolution, and the azimuth of the bounding lines of the project area. This way the cell points can be generated automatically in a programming loop. There are other approaches to rastarisation as discussed by [7], especially when the project area is irregularly shaped.

Basically, we want to trace a ray from the desired ground point through the camera lens to the image pixel using the direct equations. The orientation parameters of the linear array image are different on each line of imagery. Thus, camera position and attitude depend on the image line number that is still unknown at the beginning of the computation. Initial values can be set and then refined in a few iterations.

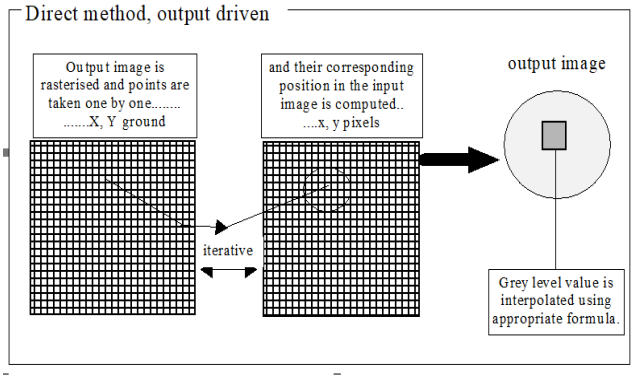

Figure 6: Direct method ortho-computation

These initial approximate pixel co-ordinates could be calculated with linear transformation parameters calculated with the aid of a few GCPs. Since this transformation is also calculated during the geometric modelling computation, the parameters could be loaded with the orientation results and used here to get the approximate line number. Empirical tests by [8] show that where the approximate image co-ordinates are chosen at the centre of the scene, the system still converges rapidly. Updated orientation parameters are used with the ground co-ordinates and the collinearity formula to compute new (and eventually final) pixel coordinates.

Using the rotation matrix,

$$R = \begin{bmatrix} r_{11} & r_{12} & r_{13} \\ r_{21} & r_{22} & r_{23} \\ r_{31} & r_{32} & r_{33} \end{bmatrix} = \begin{bmatrix} \mathbf{r_1} \\ \mathbf{r_2} \\ \mathbf{r_3} \end{bmatrix} \quad (25)$$

the shift vector,

$$D = \begin{bmatrix} \mathbf{d_1} \\ \mathbf{d_2} \\ \mathbf{d_3} \end{bmatrix} = \begin{bmatrix} Xg - Xp \\ Yg - Yp \\ Zg - Zp \end{bmatrix} \quad (26)$$

the direct equations and employing vector dot product, the direct equations can be re-written in this form:

x-image $= 0 = (\mathbf{r_1} \bullet D) / (\mathbf{r_3} \bullet D)$ (27)

and y-image $= (\mathbf{r_2} \bullet D) / (\mathbf{r_3} \bullet D)$ (28)

Since x-pixel co-ordinates used in the collinearity system for linear array imagery is always zero, the results of each iteration of this resection would be corrections to the actual approximate x-pixel co-ordinates and new y-pixel co-ordinates. These are used in the next iteration until the differences between calculated and approximate pixel co-ordinates become negligible. The final pixel co-ordinates will not be whole numbers, therefore grey levels would have to be transferred into the output image using appropriate interpolation formula, for example, nearest neighbour or bi-linear interpolation.

Below is the algorithm for the output driven system where the definition of the target area is in a ground coordinate system.

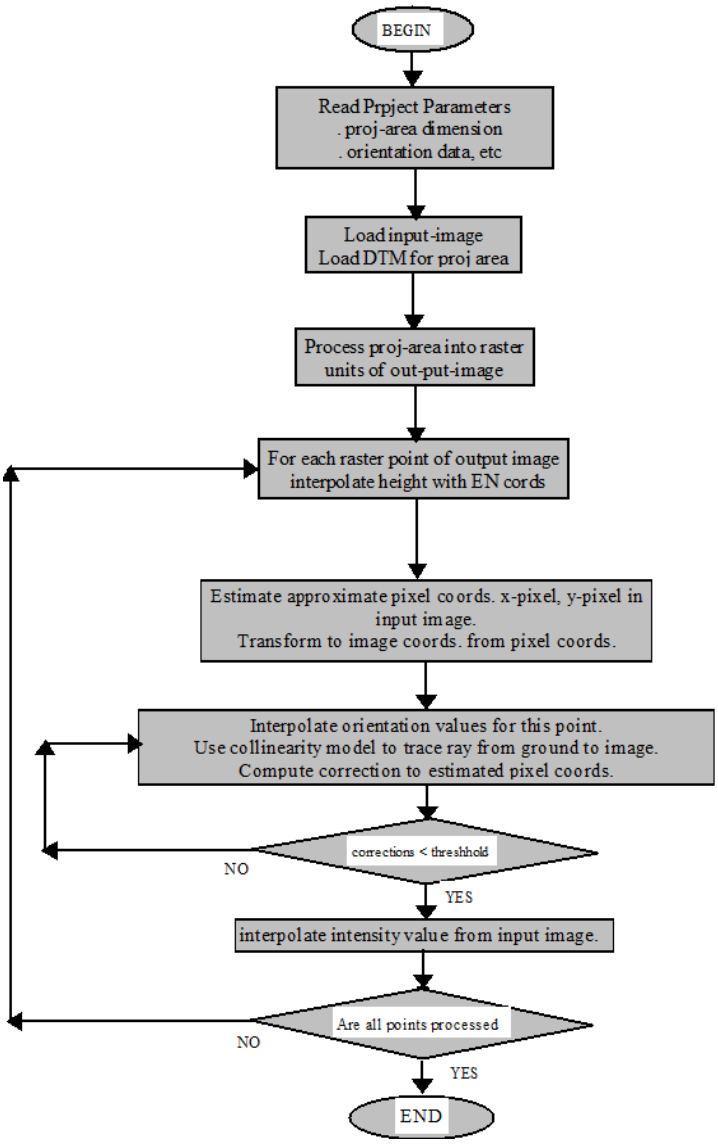

Figure 7: Schematic diagram for ortho-image generation

VI. REAT TIME PROGRAM (RTP) - ONLINE ASPECTS

Contour lines computed from DEMs tend to lack critical terrain brake-line features. That is why contours traced out in a stereo model are unique and would usually be stored separately in a geographical database. This is a major motivation for supporting stereo-panning systems, even in this era dominated by 3D laser (and LIDAR) scanning with terrain features extracted via mono-plotting from ortho-rectified satellite imagery.

Online model panning of linear array imagery is complicated due to difficulties in generating eppipolar imagery of linear array imagery [9]. In processing aerial photography, eppipolar principle is quite simple to apply and is regularly employed in RTP systems.

In implementing online model panning, it is considered that the central processing unit (CPU) now must cope when with the need to support congruent, concurrent image display in a real time program. It could be specified that 40% of computing resources be used to service this image superimposition sub-system of the Real Time Programme (RTP).

A. COPLANARITY CONSIDERATIONS

Collinearity places the exposure station, the imaged point, and the image point on a straight line [10] – which we say is likely cured a bit – because of lens imperfections and atmospheric effects. Coplanarity requires that the imaged point, its two imaged points on a stereopair images, and their two exposure lens centres all lie in a common plane.

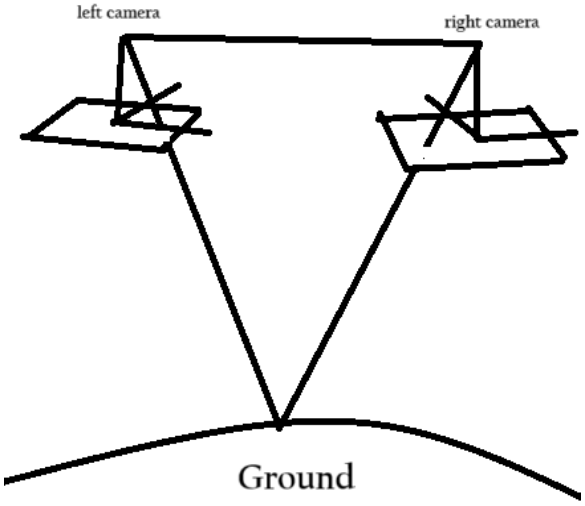

Figure 8: Coplanarity Condition

Coplanarity is not of great consideration with linear array imaging as relative orientation is not a major production line, except for those cases where stereo model panning is desired, for example to manually extract elevation contour lines and map features.

A. KEY ISSUES IN REAL TIME PROGRAMMING (ON-LINE ASPECTS)

A real time analysis of SPOT has been done by [11] and could be modified for any other dynamic imaging system like airborne ASAS. For clarity, the 'model' system refers to the co-ordinate system in which the orientation is calculated, and for ASAS this is a local Geodetic system, for SPOT this would be the inertial geocentric system. **x'y'** refer to the left image co-ordinates, and **x"** and **y"** refer to the right image co-ordinates.

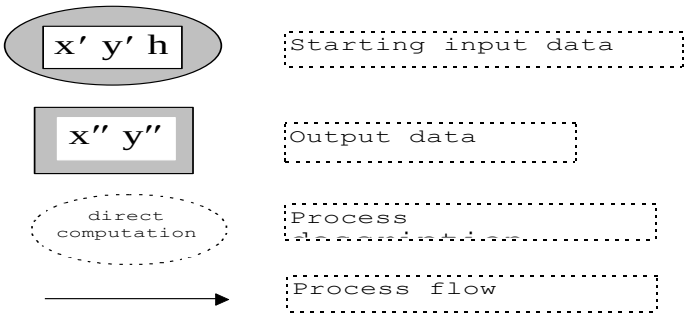

Real time model panning on a photogrammetric stereo-plotter requires that the model position on the stereo-images be updated at a high frequency. There were earlier suggestions [11] that the required frequency should be above 50 Hz, but operational systems [8] have shown 25 Hz to be adequate.

The orientation parameters of a dynamic systems change with time and is different for every scan-line (x-image co-ordinate). An RTP for the dynamic SPOT or ASAS model, if driven by encoder-input in ground units, would require an iterative computation because the x-image co-ordinates are required (and not known) to derive the orientation parameters.

Procedure 1: Conventional approach

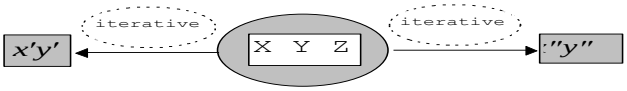

This requires many iterations and, therefore, takes too long. This could require even more iterations for airborne imagery because their platforms are more unstable.

In six iterations, this could result in more than 500 floating point multiplication (FPs) per image which is about 20 times the required number in a perspective RTP system. This would be difficult to achieve, after allocating resources to other computing tasks, on typical CPUs of the day. The number of FP calculations are less for airborne imagery because of the absence of transformations between the inertial system and the local co-ordinate system. With a high-end workstation this procedure is adequate for air-borne linear array imagery, especially if the orientation system uses INS measurements of attitude. With frequent, accurate attitude data, the non-systematic turbulent motion of an airborne platform is reconstructed. A solution based on only GCPs relies on a systematic fit of orientation parameters and would benefit more from the use of polynomials - Rational Polynomial Coefficients (RPCs) as per [12] See procedures 2 and 3 below for model panning.

A stereo-plotter operator expects a seamless integration, so working with the SPOT or ASAS model, for example, should feel the same as a model based on the perspective geometry of conventional aerial photography. Thus, model-movement digitiser input-devices must respond in similar fashion and the floating measuring mark should move in the same consistent direction when the model-movement input-devices are triggered, for example when the trackball is turned in a certain direction. Model co-ordinates drive RTPs for conventional photogrammetric models with the axis almost aligned to the photo co-ordinate system. To achieve the same effect, image co-ordinates would be the logical choice of model-movement input for a linear array RTP system. There may be a re-direction of X- and Y-axis from the expected movement of the floating mark because the presentation of images in the stereo-plotter depends on whether you have across- or along-track stereo imaging. For example, across-track stereo like SPOT requires a different alignment of conjugate imagery compared to a long-track stereo like JERS – see [13]. This reverse transformation to exchange X- and Y- axes should be computed apriori (after orientation) and incorporated in the RTP and preferably stored in a 2 x 2 matrix.

Accordingly, the operator expects the floating mark to move at right-angles to the plate when the foot disk (or equivalent device) is displaced as is the situation in the model of conventional photography. This requires that the height (h) be the choice of input for the third encoder. This height should refer to the local geodetic system and would, therefore, compound the implementation in space-borne systems whose orientation is computed in the inertial geocentric system.

Another approach is to have encoder input in x' y' h. The height allows for scale to be solved in the collinearity model and thus the transformation to the model system is accomplished in one step without iterations. Then the calculation of x"y" proceeds iteratively (see procedure 2 below). Doing these computations in single precision would save computing time but is no longer encouraged. Though less than 300 FP calculations per cycle are needed here, this may still not be fast enough.

Procedure 2: One-step optimisation for Space-borne imagery

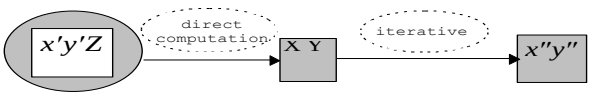

This is faster but the Z-floating mark may not move vertically to the image plane.

A further optimisation for airborne linear array imagery is to have the encoder input-devices driven by **x'y'h** but to compute two polynomials linking **x'y'h** to Eastings, and Northings (EN). This could be done using three levels of H from a 5 x 5 grid covering the whole left image (see procedure 3 below). Space-borne imagery, e.g. SPOT, would require a third polynomial linking **x'y'h** to the Z-geocentric co-ordinates. Note that the Z-co-ordinates are virtually the same in both the inertial geocentric (ECI) and the Earth's geocentric (ECEF) co-ordinate systems.

Procedure 3a: polynomial fit for Space-borne systems

This is the drill for computing ENh values for a 5x5 SPOT grid for a chosen height (h).

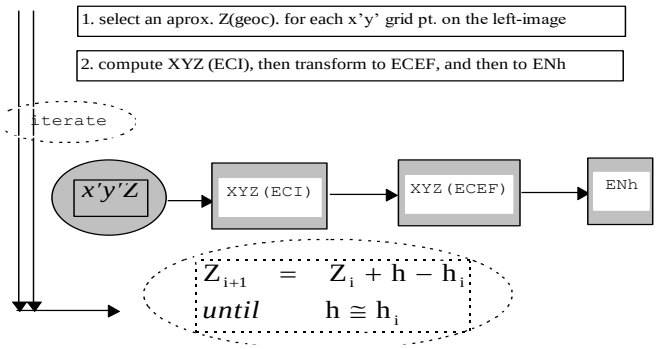

Airborne models relying only on GCPs (no INS) could benefit from using similar polynomials. The parameters of orientation systems relying on INS will not easily fit into a polynomial, therefore computational optimisation for RTP may not be pursued there.

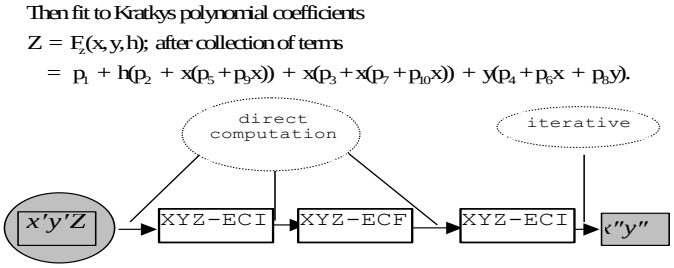

This should work well but can still be further optimised

Procedure 3b: Polynomial fit for airborne systems

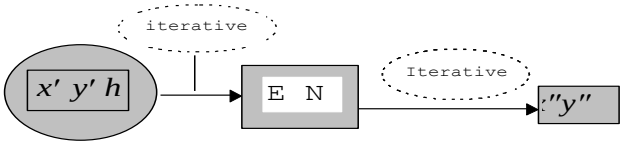

Select a 5x5 grid of image coords and 3 levels of height (h).

for each x'y' grid-point on the left image,
compute ENh values

Then fit to Kratkys polynomial coefficients

$E = F_E(x, y, h)$; after collection of terms

$= p_1 + h(p_2 + x(p_5 + p_9 x)) + x(p_3 + x(p_7 + p_{10} x)) + y(p_4 + p_6 x + p_8 y)$.

$N = F_N(x, y, h)$;

$= p_1 + h(p_2 + x(p_5 + p_9 x)) + x(p_3 + x(p_7 + p_{10} x)) + y(p_4 + p_6 x + p_8 y)$.

This should work well but can still be further optimised

[11] has presented two suitable third-degree polynomials, one for either Eastings or Northings (with 13 parameters), and the other for the Z-geocentric co-ordinates (with 10 parameters); simulations have shown that these are fairly accurate [8]

VII. CONCLUSION

Computational set-up for ortho-image and real time model panning for spaceborne and airborne linear array imagery require attention to detail in choosing from optional algorithms. For ortho-image computation for visualisation projects you use the input driven approach, while for mapping you use the output driven approach.
For both ortho-imaging and real-time model panning, there are optional that mitigate computational limitations.

REFERENCES

1. A. G. Nwosu and J-P. Muller, "Technical specifications for a Camera Model for the NASA-Advanced Solid-State Array Spectroradiometer (ASAS)", Proceedings of ASPRS/ ACSM Convention, Monitoring and Mapping Global Change, Washington D.C. 3-7 Aug. 1998, pp. 364-373.
2. D. J. Gugan and I. J. Dowman, "Topographic Mapping from SPOT Imagery", Photogrammetric Engineering and Remote Sensing, Vol. 54, No. 10, October 1988, pp. 1409-1414.
3. T. Westin, "Precision Rectification of SPOT Imagery", Photogrammetric Engineering and Remote Sensing, Vol. 56, No. 2, 1990, pp. 247-253.
4. E. M. Mikhail, - with contributions from Ackermann F, Observations and Least Squares, New York: EIP; xi, 497 pages, 1976.
5. A. Tuladhar and B. Makarovic, "Upgrading DTMs from Contour Lines Using Photogrammetric Selective Sampling", ITC Journal 1988-4.
6. B. Markarovic, "Digital Monoplotting", ITC Journal 1973-4.
7. dG. Konecny, "Geometric Evaluation of SPOT Imagery". CERCO seminar on the SPOT system and its applications, Paris, September 6-9, 1988, pp. 20-53.
8. A. G. Nwosu and A. Meid, "The Leica System for Orientation of Linear array Sensor Imagery", Proceedings of ISPRS Congress, Vienna, Aug. 1996.
9. K. L. A. 20
10. , "Simulated Photogrammetric Data for Testing the Performance of Photogrammetric Instruments and Systems", International Journal of Innovation Scientific Research and Review, Vol. 12, No. 5, 9357-9363, 2022.
11. E. Q. Rosado, Introduction to Applied Photogrammetry and Cartography for Civil Engineering, Universidad de Extremadura. I.S.B.N. 978-84-09-00910-7, 2018.
12. V. Kratky, "Rigorous Stereo-photogrammetric Treatment of SPOT Images", Photogrammetric Engineering and Remote Sensing, vol. 55, No. 3, pp. 311-316, March 1989.
13. G. Zhou, X. Li, T. Yue, W. Huang, C. He, and Y. Huan, "Solving the Rational Polynomial Coefficients Based On L Curve", The International Archives of the Photogrammetry, Remote Sensing and Spatial Information Sciences, Volume XLII-3, 2018.
14. [R. J. Wicherson, "Photogrammetric Potential of JERS-1 OPS", ISPRS XVIII Congress, Vienna, 1996.